Proceedings of the International Conference on Oxide Materials for Electronic Engineering (OMEE 2021)

Optimal Vector Phase Matching for Second Harmonic Generation in Orthorhombic Non-Linear Optical Crystals

O. Buryy[a,*], N. Andrushchak[b], A. Danylov[c], B. Sahraoui[d] and A. Andrushchak[c]

[a] *Department of Semiconductor Electronics, Lviv Polytechnic National University, 12 Bandery str., 79013 Lviv, Ukraine*
[b] *Department of Computer-Aided Design Systems, Lviv Polytechnic National University, 12 Bandery str., 79013 Lviv, Ukraine*
[c] *Department of Applied Physics and Nanomaterials Science, Lviv Polytechnic National University, 12 Bandery str., 79013 Lviv, Ukraine*
[d] *University of Angers, MOLTECH-Anjou Laboratory, MR CNRS 6200, 2 bd Lavoisier, 49045 Angers, France*

Doi: 10.12693/APhysPolA.141.365 *e-mail: oleh.a.buryi@lpnu.ua

Optimal geometries of vector phase matching are determined for the second harmonic generation in biaxial non-linear optical crystals of orthorhombic symmetry — CBO, LRB4, LBO, KB5, $KNbO_3$, KTA, KTP. The directions of wave vectors ensuring the highest possible efficiency of the second harmonic generation are defined by the extreme surface method. It is shown, that the increase of the second harmonic generation efficiency (tens to hundreds per cent) provided by the realization of vector phase-matching conditions compared to the case of the scalar ones takes place for CBO, LRB4, KB5, $KNbO_3$, KTA and KTP crystals.

topics: second harmonic generation, biaxial crystals, phase matching, extreme surfaces

1. Introduction

Second harmonic generation (SHG) in non-linear optical media attracts attention of researches for recent decades. This effect is widely used to obtain coherent light with wavelength shorter than the primary source [1–3]. The efficiency of SHG in crystals strongly depends on the directions of pump (initial) and second harmonic (output) beams. Thus, to ensure the highest possible efficiency, determination of their optimal directions should be carried out. This problem poses no difficulties for uniaxial non-linear optical crystals and scalar phase matching (SPM) [4]. However, the problem is complicated for biaxial crystals, and especially vector phase matching (VPM), when the directions of the wave vectors of the pump and SH beams do not coincide. Although the efficiency in the case of the VPM is limited by relatively low length of the interaction region due to the non-collinearity of the pump beams, the wide variety of possible directions may lead to a significant increase of the conversion efficiency. To determine the directions of the pump and SH beams corresponding to the highest SH efficiency in biaxial non-linear optical crystals, here we use a previously developed technique based on the construction and analysis of extreme surfaces to optimize the geometry for optical effects (i.e., determining the optimal directions of light beams, acoustic wave, electrical field etc.) [5–7] and expanded further on the case of non-linear optical effects in uniaxial media [8]. Optimization is performed for a number of frequently-used non-linear biaxial optical crystals of orthorhombic syngony.

2. Basic relations

The main relations used for the analysis were given in [8]. To take into account only the dependence of the SHG efficiency on the directions of the light beams, we consider the geometrical factor of the efficiency

$$\eta = \frac{\left(\boldsymbol{e}_3\, \hat{d}\, \boldsymbol{e}_1 \boldsymbol{e}_2\right)^2}{n_1\left(\lambda_p\right) n_2\left(\lambda_p\right) n_3\left(\lambda_{\mathrm{SH}}\right)}. \tag{1}$$

Here $\hat{d}$ is the non-linear susceptibility tensor, $\boldsymbol{e}_1$, $\boldsymbol{e}_2$, $\boldsymbol{e}_3$ are the unit vectors parallel to the electric vectors of the corresponding waves determined for each direction of the wave vector $\boldsymbol{k}$ in a known manner (see, e.g. [4]), while $n(\lambda_1)$, $n(\lambda_2)$, $n(\lambda_3)$ are their refraction indices. Next λ_p is the pump beams wavelength, λ_{SH} is SH beam wavelength ($\lambda_{\mathrm{SH}} = 0.5\lambda_p$), $n_{1,2}(\lambda_p)$, $n_3(\lambda_{\mathrm{SH}})$, are refraction indices at the corresponding wavelength. In the case of SPM, $n_1(\lambda_p) = n_2(\lambda_p)$. For ease of description, we will refer to η as "efficiency". Now, (1) is used for the construction of the extreme surfaces representing the highest achievable values of η for all possible directions of the output wave vector $\boldsymbol{k}_3$, determined by the angles θ, ϕ of the spherical coordinate system.

As it is known, the highest SH efficiency is achieved when the phase-matching (PM) condition is realized. Its general form is

$$\boldsymbol{k}_3 = \boldsymbol{k}_1 + \boldsymbol{k}_2, \tag{2}$$

where $\boldsymbol{k}_1$, $\boldsymbol{k}_2$ are the wave vectors of the pump beams with the frequency ω, and $\boldsymbol{k}_3$ is the wave vector of the SH beam with the frequency 2ω. For scalar PM (SPM), (2) comes to the relationship between the absolute values of the wave vectors.

Generally, two orthogonal polarization light waves can propagate in an anisotropic crystalline material for each direction. In the case of biaxial crystal, the lengths of the wave vectors of these waves $k = |\boldsymbol{k}|$ are determined using [4]

$$\begin{aligned} & k^4\left(K_1^2 m_1^2 + K_2^2 m_2^2 + K_3^2 m_3^2\right) \\ & -k^2\left[K_1^2\left(K_2^2 + K_3^2\right) m_1^2 + K_2^2\left(K_1^2 + K_3^2\right) m_2^2\right. \\ & \left. +K_3^2\left(K_1^2 + K_2^2\right) m_3^2\right] + K_1^2 K_2^2 K_3^2 = 0, \end{aligned} \tag{3}$$

where K_1, K_2, K_3 are the lengths of the wave vectors along crystallographic axes, $K_i = 2\pi N_i/\lambda$ ($i = 1, 2, 3$), N_i are the main refraction indices, and m_1, m_2, m_3 are the components of the wave normal. Here (3) describes the wave vector surface with a double cavity (Fig. 1). The external part of this surface corresponds to a "slow" (s) wave characterized by a higher value of the refraction index n and, consequently, a higher absolute value of the wave vector $k = 2\pi n/\lambda$, and the internal part of the surface — to the "fast" (f) wave. For biaxial crystals, the PM condition (2) can be satisfied in two possible cases: (i) both pump waves are slow (ssf or type I phase matching) or (ii) one pump wave is slow and the other is fast (sff or type II phase matching) [3]. In both cases, the SH wave is the fast one.

The analysis of the scalar phase-matching conditions for biaxial crystals has been carried out in a number of papers (see, e.g [9–11]), but the general case of the vector PM has not yet been analyzed. Considering the VPM is significantly complicated by the fact that for each direction of $\boldsymbol{k}_3$, the PM condition (2) can be satisfied for different directions of $\boldsymbol{k}_1$, $\boldsymbol{k}_2$ (Fig. 2). Generally, different values of the efficiency η correspond to different $\boldsymbol{k}_1$, $\boldsymbol{k}_2$ (for the same $\boldsymbol{k}_3$). To determine the maximum value, $\eta_{\max}$, the values of η should be calculated for all $\boldsymbol{k}_1$, $\boldsymbol{k}_2$ (certainly, with a small enough step) forming the cone in Fig. 2. Notably, all possible vectors $\boldsymbol{k}_1$ are finished and all possible vectors $\boldsymbol{k}_2$ start with the line C which points can be determined in the following way. Let the wave vector $\boldsymbol{k}_3$ is known and, for certainty, the type I (ssf) PM is considered. In this case both wave vectors $\boldsymbol{k}_1$ and $\boldsymbol{k}_2$ are finished on the external part of the wave vector surface. Let's shift the surface corresponding to the wave vector $\boldsymbol{k}_2$ to the end of the wave vector $\boldsymbol{k}_3$. Now the surfaces for the wave vectors $\boldsymbol{k}_1$ and $\boldsymbol{k}_2$ intersect along the closed line C, each point of which corresponds to the ends of vectors $\boldsymbol{k}_1$ and $\boldsymbol{k}_3 + \boldsymbol{k}_2$ (if this intersection is absent, the PM can not be achieved for considered wavelengths and type of phase matching). Because the inversion of the wave vector $\boldsymbol{k}_2$ does not change the polarizations of the light beams, this line corresponds to the condition (2). In our analysis, the Dragilev' method (see Appendix in [12]) was used to determine this line. The determination of the line C is described in more detail in [8] for the case of uniaxial non-linear optical crystals.

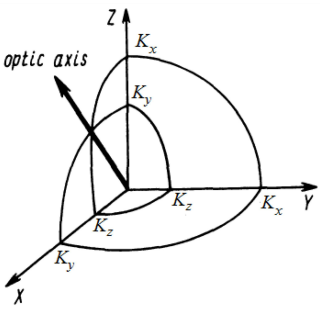

Fig. 1. One-eighth part of the wave vector surface for the case of biaxial crystal.

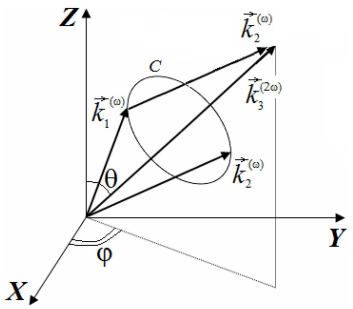

Fig. 2. The mutual position of the wave vectors of pump and SH beams.

If the maximal efficiency $\eta_{\max}$ was determined for all possible SH wave vector directions (determined by the angles of spherical coordinate system θ, ϕ; as usual $\theta = 0 \ldots \pi$, $\phi = 0 \ldots 2\pi$), the global maximal value of the efficiency $\eta_{\max}^{\mathrm{extr}}$ can be obtained as the highest value from the set of the $\eta_{\max}$ values determined for all $\boldsymbol{k}_3$. The dependence $\eta_{\max}(\theta, \varphi)$ is conveniently presented as a 3D surface (extreme

TABLE I

Parameters of considered crystals.

Crystal	Wavelengths and main refraction indices							Non-linear susceptibilities d_{ij} [pm/V]
	λ_p [μm]	Pump beams			SH beam			
		N_1	N_2	N_3	N_1	N_2	N_3	
Point group 222								
CsB_3O_5 (CBO)	1.0642	1.5196	1.5494	1.5770	1.5336	1.5682	1.5958	$d_{14} = d_{36} = d_{25} = 1.49$
$LiRbB_4O_7$ (LRB4)	1.0642	1.5018	1.5225	1.5342	1.5157	1.5414	1.5473	$d_{14} = d_{36} = d_{25} = 0.45$
Point group mm2								
LiB_3O_6 (LBO)	1.0642	1.5648	1.5904	1.6053	1.5785	1.6065	1.6216	$d_{15} = -0.67$; $d_{24} = 0.85$; $d_{31} = -0.67$; $d_{32} = 0.85$; $d_{33} = 0.04$
$KB_5O_8{\cdot}4H_2O$ (KB5)	0.5321	1.4889	1.4359	1.4233	1.5317	1.4759	1.4637	$d_{15} = 0.04$; $d_{24} = 0.003$; $d_{31} = 0.04$; $d_{32} = 0.003$; $d_{33} = 0.05$
$KNbO_3$	1.0642	2.2575	2.2194	2.1195	2.3816	2.3225	2.2031	$d_{15} = -12.4$; $d_{24} = -12.8$; $d_{31} = -11.9$; $d_{32} = -13.7$; $d_{33} = -20.6$
$KTiOAsO_4$ (KTA)	1.0642	1.7891	1.7928	1.8679	1.8294	1.8357	1.9311	$d_{15} = 2.5$; $d_{24} = 4.4$; $d_{31} = 2.9$; $d_{32} = 5.1$; $d_{33} = 16.2$
$KTiOPO_4$ (KTP)	1.0642	1.7379	1.7455	1.8297	1.7779	1.7887	1.8886	$d_{15} = 1.9$; $d_{24} = 3.7$; $d_{31} = 2.2$; $d_{32} = 3.7$; $d_{33} = 14.6$

in accordance to its calculation method). Here we construct such surfaces and determine the optimal PM conditions for a number of orthorhombic nonlinear optical crystals which parameters are given in Table I. The values of the parameters are taken from [3, 13], in particular, the refraction indices were calculated in accordance with Sellmeier equations given in these papers. The pump beams wavelengths are equal to 1.0642 μm for all crystals, except for KB5 where the pump beams with shorter wavelengths are used for SHG [13]. The transformation of the axes from the crystallographic coordinate system (abc) to the crystal-optics system (XYZ) were carried out in accordance with the rules given in [3, 11]:

- $XYZ \leftrightarrow cab$ (CBO crystal),
- $XYZ \leftrightarrow bca$ (LRB4),
- $XYZ \leftrightarrow acb$ (LBO),
- $XYZ \leftrightarrow abc$ (KB5, KTA, KTP),
- $XYZ \leftrightarrow bac$ ($KNbO_3$).

Note that all extreme surfaces were constructed in crystal-optics coordinate system.

3. Results and discussion

The general and the top views of the extreme surfaces of the SHG efficiency $\eta_{\max}$ for the investigated crystals are shown in Figs. 3 and 4. The black lines correspond to the scalar PM conditions. Because the type II PM can not be achieved in KB5, $KNbO_3$, KTA crystals for the considered wavelengths, only one extreme surface is shown for each of them. The results of optimization are given in Tables II and III where, for brevity, the position of only one of the equivalent maxima for each crystal is indicated. In the last columns in Tables II and III, the relative increase of the efficiency

$$\kappa = \frac{\eta_v^{\text{extr}} - \eta_{sc}^{extr}}{\eta_{sc}^{\text{extr}}} \times 100\% \qquad (4)$$

caused by the use of the vector PM in comparison with scalar one is given (in brackets). Here, η_v^{extr} and η_{sc}^{extr} are the highest achievable values of the efficiency in the VPM and SPM cases, respectively.

As it is seen in Figs. 3 and 4, the forms of the extreme surfaces for crystals of the same point group are usually not similar (such similarity is observed only for the case of ssf PM in KTA and KTP, and, to some extent, for CBO and LRB4). This is obviously due to different rules of coordinates transformation and different relationships between the values of non-linear susceptibilities d_{ij}. Note that the extreme surfaces for ssf PM in KTA and KTP do not have the symmetry axes of 4th order as it can be mistakenly concluded from Fig. 4. In particular, for the KTA crystal, the angle in the XY plane between the directions corresponding to the maxima of $\eta_{\max}$ is equal to 93.5° between the "petals" placed in the first and second, as well as in the third and forth octants. Correspondingly, the angles between the "petals" placed in the second

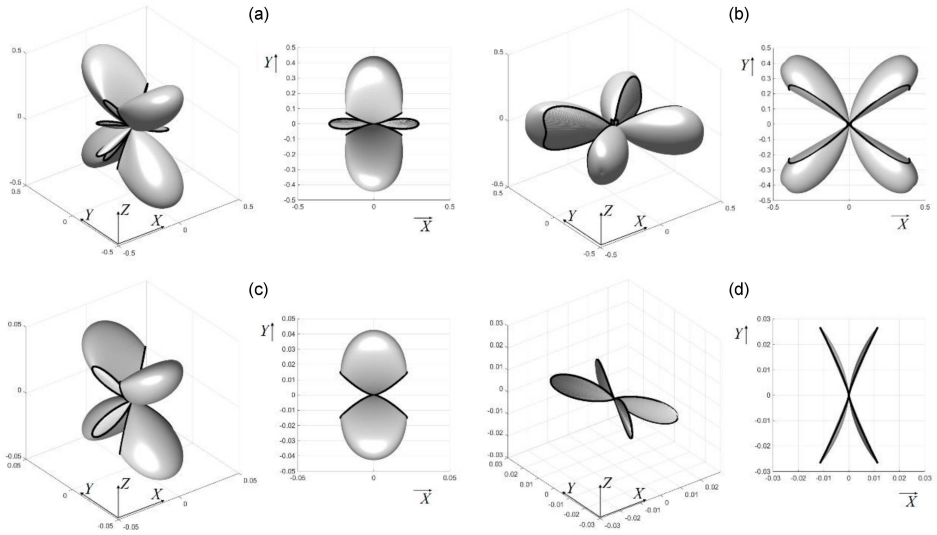

Fig. 3. The extreme surfaces $\eta_{\max}(\theta, \phi)$ [pm^2/V^2] for VPM in crystals of 222 symmetry: (a) ssf CBO, (b) sff CBO, (c) ssf LRB4, (d) sff LRB4.

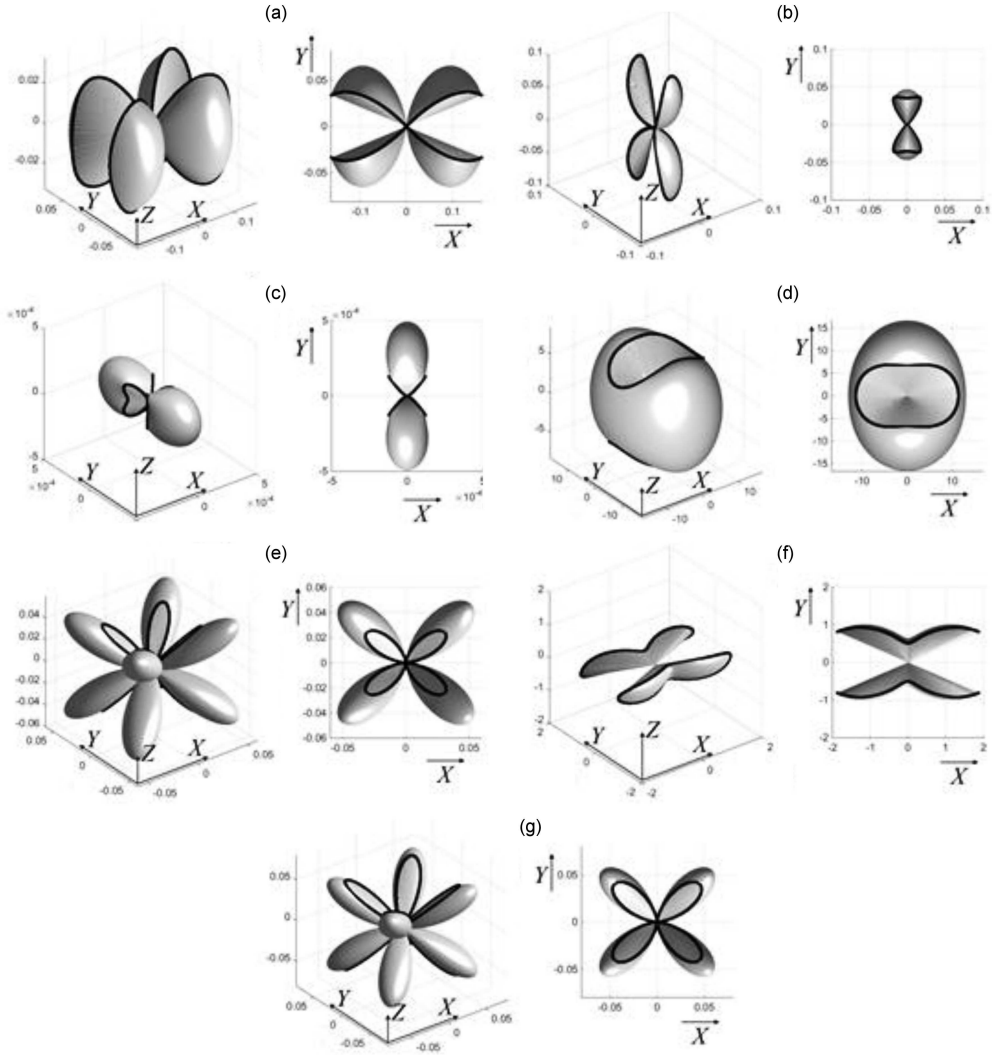

Fig. 4. The extreme surfaces $\eta_{\max}(\theta, \phi)$ [pm^2/V^2] for VPM in crystals of mm2 symmetry: (a) ssf LBO, (b) sff LBO, (c) ssf KB5, (d) ssf $KNbO_3$, (e) ssf KTP, (f) sff KTP, (g) ssf KTA.

TABLE II

Results of optimization (type I PM, ssf).

Crystal	Phase matching							
	Scalar			Vector				
	Angles [deg]		η_{sc}^{extr} [pm^2/V^2]	Angles [deg] (pump beams)		Angles [deg] (SH beam)		η_v^{extr} [pm^2/V^2] (κ)
	θ	ϕ		θ_p	ϕ_p	θ	ϕ	
CBO	112.5	0	0.32	56.9	90	45.7	90	0.59 (84%)
				34.5	90			
LRB4	44.9	213.7	0.037	37.9	90	45.2	90	0.057 (54%)
				52.6	90			
LBO	89.9	168.4	0.17	coincides with SPM				
KB5	121.4	133.4	2.0×10^{-4}	100.6	90	90	90	4.9×10^{-4} (145%)
				79.4	90			
$KNbO_3$	71.4	0	12.0	102.6	90	90	90	16.7 (39.2%)
				77.4	90			
KTA	131.6	42.1	0.081	118.7	141.2	123.5	136.8	0.095 (17.3%)
				128.2	131.7			
KTP	134.7	218.4	0.055	116.0	36.3	122.7	41.7	0.082 (49%)
				129.3	48.1			

TABLE III

Results of optimization (type II PM, sff).

Crystal	Phase matching							
	Scalar			Vector				
	Angles [deg]		η_{sc}^{extr} [pm^2/V^2]	Angles [deg] (pump beams)		Angles [deg] (SH beam)		η_v^{extr} [pm^2/V^2] (κ)
	θ	ϕ		θ_p	ϕ_p	θ	ϕ	
CBO	76.7	147.1	0.48	90	127.6	90	133	0.59 (23%)
				90	138.6			
LRB4	69.1	109.7	0.054	coincides with SPM				
LBO	20.5	90	0.10	coincides with SPM				
KB5	phase matching is absent							
$KNbO_3$	phase matching is absent							
KTA	phase matching is absent							
KTP	90	156.6	2.0	coincides with SPM				

and third, forth and first octants is 86.5°. The same angles for the KTP crystal are 96.5° and 83.5°, so the extreme surfaces do not reveal the symmetry higher than orthorhombic.

For some crystals (KB5, $KNbO_3$, KTA), the sff PM conditions are not fulfilled for the considered wavelengths. Also, as it is followed from our calculations, the use of type I (ssf) VPM does not allow to increase the efficiency η compared to the case of SPM for LBO crystals. In these cases, in Fig. 3, the lines corresponding to SPM frame the edges of the extreme surfaces and pass through the points corresponding to η_v^{extr}. The same situation takes place in the case of type II (ssf) VPM in LRB4, LBO and KTP (Table III). In other cases the increase of the SHG efficiency ensured by ssf vector PM is equal to 84% for CBO, 54% for LRB4, 145% for KB5, 49% for KTP, 39% for $KNbO_3$ and 17% for KTA crystals, whereas for sff VPM in CBO it is remarkably lower (23%). Thus, in some instances, especially for ssf phase matching, the use of the vector PM allows to obtain significantly higher efficiencies than the use of scalar, indicating a possible way to enhance the performance of non-linear optical devices.

4. Conclusions

Optimal geometries of vector phase matching were determined for second harmonic generation in biaxial non-linear optical crystals of orthorhombic symmetry — CBO, LRB4, LBO, KB5, $KNbO_3$, KTA, KTP. The directions of wave vectors ensuring the highest possible efficiency of SHG were defined by the extreme surface method. Both first (ssf) and

second (sff) type phase matching were considered. As it is shown, the highest achievable SHG efficiencies for vector PM are not higher than the ones for scalar PM in the cases of LRB4 (sff), KTP (sff) and LBO (both types of PM). Besides, sff PM is absent in KB5, $KNbO_3$ and KTA crystals at the initial beams wavelengths considered. Relative increasing of the efficiency in the case of ssf VPM is equal to 84% for CBO, 54% for LRB4, 145% for KB5, 49% for KTP, 39% for $KNbO_3$ and 17% for KTA. For sff VPM the relative increase of the efficiency is observed only for one of the investigated crystals, i.e., CBO, and amounts about 23%.

Acknowledgments

This research has received funding from the European Union's Horizon 2020 research and innovation programme under the Marie Skłodowska-Curie grant agreement No 778156 and from Ministry of Education and Science of Ukraine in the frames of projects "Nanocrystalit" (0119U002255) and "OPTIMA" (0120U102204).

References

[1] A. Yariv, P. Yeh, *Optical Waves in Crystals*, Wiley, New York 2002.

[2] Y.R. Shen, *The Principles of Nonlinear Optics*, Wiley-Interscience, New York 2002.

[3] V.G. Dmitriev, G.G. Gurzadyan, D.N. Nikogosyan, *Handbook of Nonlinear Optical Crystals*, 3rd ed., Springer Series in Optical Science, Vol. 64, Springer-Verlag, Berlin 1999.

[4] Yu. Sirotin, M. Shaskolskaja, *Fundamentals of Crystal Physics*, Imported Pubn., Moscow 1983.

[5] O. Buryy, A. Andrushchak, O. Kushnir, S. Ubizskii, D. Vynnyk, O. Yurkevych, A. Larchenko, K. Chaban, O. Gotra, A. Kityk, *J. Appl. Phys.* **113**, 083103 (2013).

[6] O. Buryy, A. Andrushchak, N. Demyanyshyn, B. Mytsyk, *Opt. Appl.* **46**, 447 (2016).

[7] A. Andrushchak, N. Andrushchak, Z. Hotra, O. Sushynskyi, G. Singh, V. Janyani, I. Kityk, *Appl. Opt.* **56**, 6255 (2017).

[8] N. Andrushchak, O. Buryy, A. Andrushchak, A. Danilov, S. Bouchta, *Opt. Mat.* **120**, 11420 (2021).

[9] J.P. Fève, B. Boulanger, G. Marnier, *Opt. Commun.* **99**, 284 (1993).

[10] G. Huo, Y. Wang, M. Zhang, *Appl. Phys. B* **120**, 239 (2015).

[11] Yu.M. Andreev, Yu.D. Arapov, S.G. Grechin, I.V. Kasyanov, P.P. Nikolaev, *Quantum Electron.* **46**, 995 (2016).

[12] O. Buryy, N. Andrushchak, A. Ratych, N. Demyanyshyn, B. Mytsyk, A. Andrushchak, *Appl. Opt.* **56**, 1839 (2017).

[13] D.N. Nikogosyan, *Nonlinear Optical Crystals: A Complete Survey*, Springer Science + Business Media, Inc., New York 2005.